A theoretical study of the initial stages of Si(111)–7×7 oxidation. I. The molecular precursor

Boris Schubert, Phaedon Avouris, and Roald Hoffmann

Citation: J. Chem. Phys. **98**, 7593 (1993); doi: 10.1063/1.465058
View online: http://dx.doi.org/10.1063/1.465058
View Table of Contents: http://jcp.aip.org/resource/1/JCPSA6/v98/i9
Published by the American Institute of Physics.

A theoretical study of the initial stages of Si(111)–7×7 oxidation. I. The molecular precursor

Boris Schubert
Department of Chemistry and Materials Science Center, Cornell University, Ithaca, New York 14853

Phaedon Avouris
IBM Research Division, T. J. Watson Research Center, Yorktown Heights, New York 10598

Roald Hoffmann
Department of Chemistry and Materials Science Center, Cornell University, Ithaca, New York 14853

(Received 25 August 1992; accepted 11 January 1993)

We have studied the initial stages of the oxidation of the Si(111) surface using extended Hückel tight-binding calculations. Due to the different dangling bond sites present on the reconstructed Si(111)–7×7 surface, one may expect more than one molecular precursor or dissociated Si–O configuration to be formed. As candidates for the main and kinetically most stable molecular precursor, structures involving O_2 associated with a single Si adatom site are proposed. Bridge structures are found to be less stable. However, dissociated species derived from bridge structures play an important role in the oxidation process. In this paper we introduce the computational approach used, and discuss the nature of the molecular precursors. In a second paper the nature of the atomic oxygen containing products and the mechanism of SiO_4 formation are discussed.

INTRODUCTION

The oxidation of silicon is one of the most important reactions in the area of microelectronic materials. Understanding this process would provide insight into the properties of the Si/SiO_2 interface, which critically affects the operation of microelectronic devices. Thus, the interaction of oxygen molecules or atoms with silicon has been studied intensively over 30 years, both experimentally[1–16] and theoretically.[17–20] Spectroscopic methods used in the oxidation studies, such as x-ray photoelectron spectroscopy (XPS), ultraviolet photoelectron spectroscopy (UPS), and high-resolution x-ray-induced Auger-electron spectroscopy (XAES), give information which is averaged over the different surface sites and the different Si–O configurations which may be present on the surface.

The above techniques have been supplemented more recently by scanning tunneling microscopy[21] (STM) and atom-resolved scanning tunneling spectroscopy (STS).[22] STM and STS provide information about individual surface sites. STM was, for example, decisive[23–25] in proving the atomic and electronic structure of the 7×7–Si(111) reconstruction, the DAS (dimer adatom stacking fault) or Takayanagi model[26] (Fig. 1).

As can be seen from Fig. 1, the reconstructed Si(111) surface contains the top layer Si atoms, so-called adatoms, second layer rest atoms (with dangling bonds which are not saturated by bonding to an adatom), corner holes, two different stacking patterns, and dimers. Oxidation of this complex structure is not going to be simple.

Theoretical calculations of the oxidation reaction are difficult since the unit cell is very large. Goddard, Redondo, and McGill[17] used the generalized valence bond method for a Si_3 cluster, saturated with H and with an O_2 placed on top. Chen, Batra, and Brundle[18] used the first principles extended tight-binding method with a six-layer slab of an *unreconstructed* Si(111) surface. Bhandia and Schwarz[19] performed semiempirical simple valence-force-field–bond-energy bond order calculations. Ciraci, Ellialtioglu, and Erkoc[20] used an empirical tight-binding method with a six double-layer slab of an *unreconstructed* Si(111) surface. They all come to somewhat different conclusions regarding the main oxygen species on the surface during Si(111) oxidation.

The experimental literature was reviewed recently and new UPS and XPS results were presented on the initial stages of the oxidation of Si(111).[15] In this study it was concluded that the dissociative adsorption of O_2 on Si(111) is preceded by a metastable precursor. This precursor involves molecular oxygen, which is stable at low temperatures, even for ~10 min at room temperature. Using several surface science techniques, Höfer *et al.*[15] came to the conclusion that this precursor is an O_2 bridging between adatom and rest atom dangling bonds.

The idea of a molecular precursor is also supported by the STM experiments.[27] Thus, the observed high site selectivity of the reaction can best be explained in terms of a site-selective formation of the molecular precursor at sites which have a high density of states at the Fermi energy. These sites are the corner-adatoms sites, particularly those in the faulted half of the 7×7 unit cell. A typical STM topograph obtained after the exposure of the 7×7 surface to 0.2 L of O_2 is shown in Fig. 2 (1 L=10^{-6} Torr s). There are two kinds of oxygen-induced sites which appear, respectively darker and brighter than the unreached Si adatom sites of the 7×7 surface.[27]

For the purpose of discussion we label the state of the reacted surface immediately following the O_2 exposure as *stage 1*. During stage 1 both molecular precursors and products containing atomic oxygen coexist. At longer times, say 1 h later, all molecular precursors have dissoci-

 0021-9606/93/097593-13$06.00

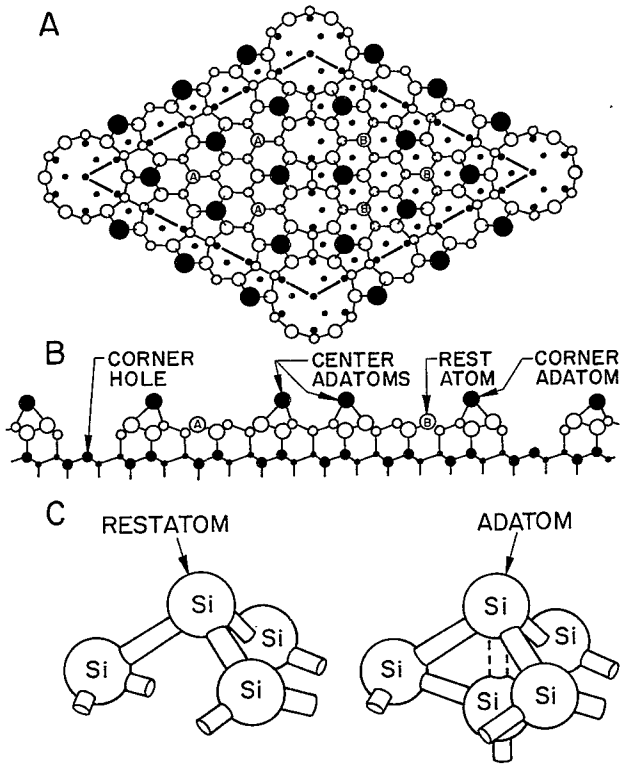

FIG. 1. (A) Top view and (B) side view of the Takayanagi, or DOS, model of the Si(111)–7×7 surface. Each unit cell contains 12 adatoms, 6 rest atoms, and one corner hole. The deeper atoms are indicated as solid dots. The left triangle shows a stacking fault. (C) Next neighbors of the rest atom and adatom site (compare also to Fig. 3).

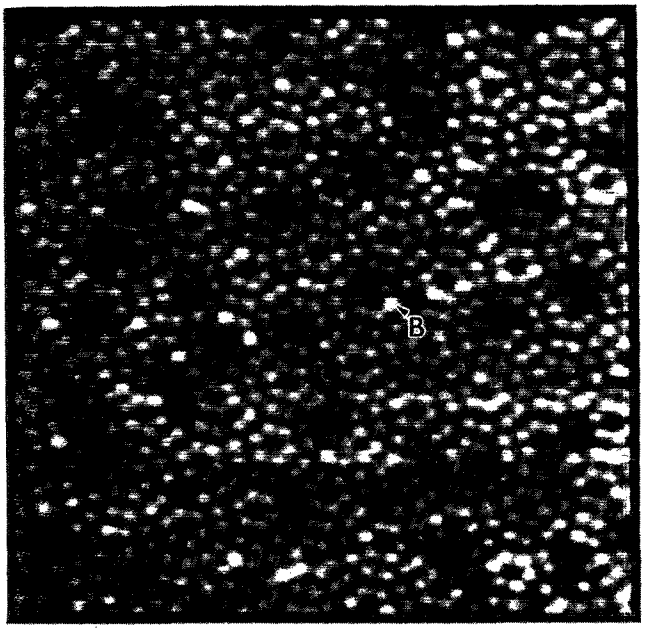

FIG. 2. Topograph of the unoccupied states of a Si(111)–7×7 surface after exposure to ~0.2 L of O_2 at 300 K (sample bias = +2 V). Typical bright oxygen-induced sites are indicated by B.

ated in a room-temperature experiment and only stable products exist. We denote this stage as *stage 2*. STM images obtained during stage 1 show time-dependent changes (e.g., certain bright sites turn dark).[27] For an exposure of ~0.2 L O_2, the site distribution is roughly 5% bright sites, 5% dark sites, and 90% unreacted sites. In stage 2 there are somewhat more dark sites than bright sites. As the O_2 exposure is increased, stage 1 becomes shorter in duration, and dark sites become the dominant products.

In this paper, we first describe our computational approach, then we briefly discuss the stable structures containing oxygen ("Si–O configurations") and finally focus on the nature of the molecular precursors. We attempt to identify the most likely precursor structures by comparing theoretical density of states (DOS) and crystal orbital overlap population[28,29] (COOP) curves with experimental UPS and STM results.

COMPUTATIONAL METHOD

We have performed extended Hückel[30] tight-binding[31] slab calculations with weighted H_{ij}'s.[32] The methodology is approximate, not reliable quantitatively, but provides a conceptual basis for understanding. Five double layers were used and the unit cell was composed of a 2×2 adatom model for the Si(111) surface which includes a rest atom. At the bottom, hydrogen saturates the dangling bonds (Si–H: 1.48 Å). Previous calculations on oxidation have used unit cells containing only an adatom; however, it has been shown[25,33] that adatoms and rest atoms are coupled, so that in order to probe charge-transfer processes both types of sites should be included. In comparison to the real 7×7 unit cell (see Fig. 1) we neglect the effect of the dimers, corner holes, and of the stacking fault. Although these, especially the stacking fault and corner holes, do play a significant role in the oxidation (see Refs. 27, 34, and 35), we think that the 2×2 unit cell is a fairly good representation for the reactive sites of the 7×7 unit cell, since adatoms and rest atoms are the dominant features of Si(111) surface chemistry.

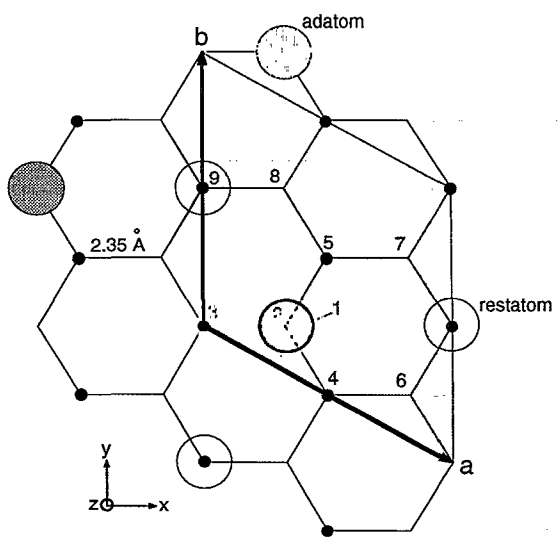

1

The 2×2 unit cell is shown in a top view in structure 1 as a slightly shadowed area on a hexagonal, puckered Si(111) surface. The numbering of the Si atoms is also indicated (the small solid circles refer to the up position). The two lattice vectors **a** and **b** of the overlayer structure are 2×3.84 Å, corresponding to the lattice vectors of the unreconstructed hexagonal Si(111) surface (3.84 Å). The large shaded circles indicate the adatoms and the large open circles indicate the rest atoms. The z direction is perpendicular to the surface.

Due to the surface reconstruction most of the surface Si atoms will be displaced from their ideal positions (Si–Si unreconstructed distance: 2.35 Å). These displacements are especially strong next to the adatom. Meade and Vanderbilt[36] have already pointed out that the adatom and the rest atom could not relax laterally since they occupy positions of threefold symmetry, and that the Si atoms 3,4,5 should relax in equal measure toward the adatom. Another aid to constructing the right atomic positions for the reconstructed Si(111) surface comes from surface x-ray diffraction studies by Robinson *et al.*:[37] The projected bond lengths into the (111) plane vary between 2.07 and 2.13 Å. Our calculations show that the bond with the most antibonding character is between Si_1 and Si_2 and should therefore be lengthened. On the other hand, the shortest bond is to be expected between Si_2 and Si_{10} (underneath Si_2 in the second double layer).

Altogether, the parameters most influenced by the reconstruction are $z(Si_1)$, $z(Si_2)$, $z(Si_{10})$ (directly underneath Si_2), $z(Si_{3,4,5})$, $r(Si_{3,4,5})$ (towards the adatom), and $z(Si_9)$. We have chosen the first set of parameters in accordance with Qian and Chadi,[38] modified slightly to take into account results from Meade and Vanderbilt[36] and from our calculations. The resulting atomic relaxations from the ideal positions are shown in structure 2 (side view). The displacements are given in 10^{-2} Å.

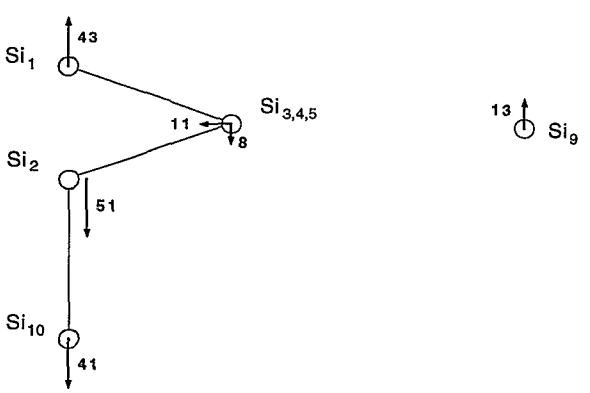

2

In our calculations we find the adatom p_z orbital and the $Si_{3,4,5}$ p_z orbitals at 0.6 eV (in the following referred to as adatom dangling bond) and the doubly occupied rest atom dangling bond at 0.7 eV (see Fig. 7).

In UPS spectra (e.g., Fig. 11) the rest atom appears at ~1 eV (previous calculations[36,38,39] have shown that the UPS peaks S_1 and S_2 derive from adatom and rest atom dangling bonds, respectively). This shift is due to the strong increase of total DOS between 0.5 and 2 eV. STS data from the rest atom site show a peak at 0.8 eV[23,24,28] in good agreement with our calculations.[40,41]

TABLE I. Summary of the extended Hückel parameters used in this contribution. The (a) H_{ii} values for oxygen are used for all Si–O configurations. In addition, we have used the (b) H_{ii} values for all configurations that do not contain molecular oxygen.

Atom	Orbital	(a) H_{ii}(eV)	(b) H_{ii}(eV)	ζ_1
O	2*s*	−30.0	−32.3	2.275
	2*p*	−13.6	−14.8	2.275
Si	3*s*	−17.3		1.383
	3*p*	−9.2		1.383
H	1*s*	−13.6		1.300

Table I summarizes the extended Hückel parameters used. The oxygen parameters were chosen as follows: By taking the energies used by Ciraci, Ellialtioglu, and Erkoc[20] [see Table I, set (a)] we find for most configurations which involve molecular oxygen a prominent peak in the DOS at 4 eV below the Fermi energy. As will be seen, this result is in agreement with the findings of photoemission experiments. For those configurations which involve *no* molecular oxygen we have used the "normal" extended Hückel parameters for oxygen [Table I, set (b)]. All solid state calculations were performed using 18 k points[42] distributed randomly over half the Brillouin zone, so as to avoid problems due to symmetry changes between different Si–O configurations.

THE SILICON–OXYGEN CONFIGURATIONS

Figure 3 shows most of the configurations discussed in this contribution. It can be seen that some involve molecular oxygen[3,5,9,15,17] either attached to one Si atom or as a bridge between two Si atoms (peroxy bridge). Other geometries are derived from adsorbing atomic oxygen on top of top-layer Si atoms[7,9,10,13] or inserting atomic oxygen into a bond between the adatom and a first layer silicon (adatom backbond).[4,6,14,15,20] In the following they are referred to as *clean* [clean reconstructed 2×2 Si(111) surface plus an oxygen molecule far away from the surface], *grif* (for Griffith),[43] *paul* (for Pauling),[44] *para* (from parallel to the surface), *trival* (one oxygen is trivalent), *bridge*, *bridge-si3*, *bridge-ins* (bridge between Si_3 and rest atom and, in addition, one oxygen is inserted), *ins* (from inserted), *ad*, *rest*, *ins-ad*, *ins-rest* (one O is inserted, one on top of the rest atom within one unit cell), and *ins-ad-rest*. In the absence of a systematic nomenclature of adsorbate sites, these terms are at least descriptive.

The sites with which the O_2 molecule interacts first, at both low and high temperatures, are the Si adatom sites. The evidence for this comes from UPS measurements, which we will show later in this paper. Rest atom sites are less reactive initially. The difference in reactivity between these two kinds of sites can be understood by considering that the initial event in the O_2 sticking to the surface in-

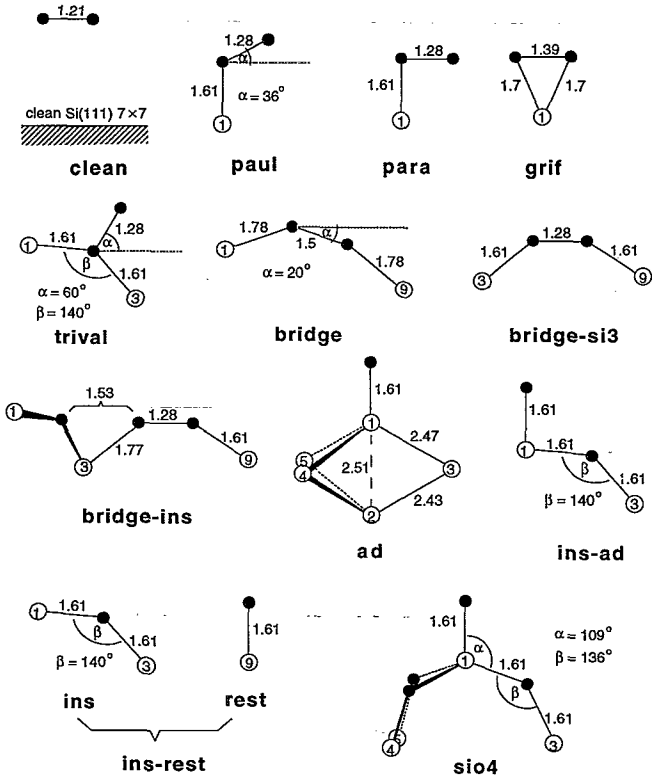

FIG. 3. The Si–O configurations discussed in this contribution (solid circle: O; open circle: Si). Si_1 is the adatom, Si_9 is the rest atom (see also Fig. 1). *Clean* stands for the clean Si(111) surface plus one O_2 molecule without any interactions with the surface. *Ins-ad-rest* (the only structure not shown) consists of *ins-ad* and *rest* in one unit cell. For *ad*, also a bit of the Si arrangement close to the adatom is displayed.

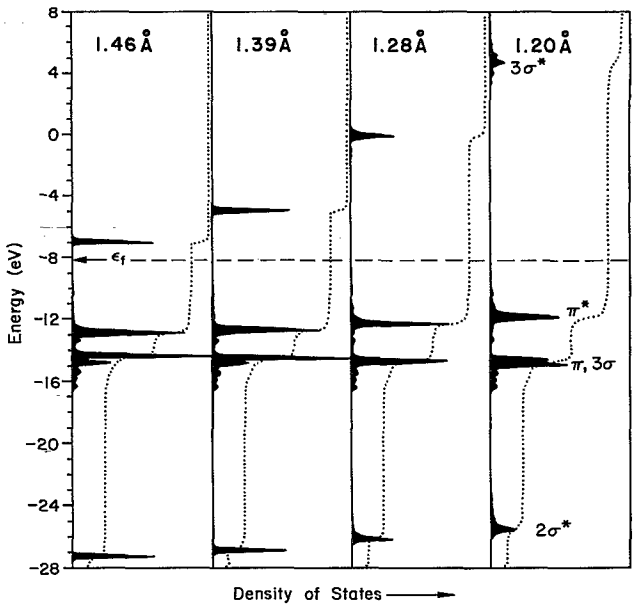

FIG. 4. Influence of the O–O distance on the oxygen DOS level splitting. Oxygen DOS for *paul* for an oxygen distance of 1.2, 1.28, 1.39, and 1.46 Å. The DOS of the bonding *s–s* interaction (2σ, not shown here) moves from −33.8 (1.46 Å) to −35.5 (1.2 Å). The integration line goes from 0% to 100% within each box.

volves a "harpooning" process in which electrons tunnel out of dangling bond states into the $2\pi^*$ affinity level of O_2.[27] The fact that the adatoms are situated more than 1 Å further out than the rest atoms, and the binding energy of their dangling bond electrons is lower than that of rest atoms, makes the harpooning process more efficient at adatom sites. This is the reason why we concentrate our initial discussion on the adatoms.

In those cases where an oxygen inserts in the adatom backbond, the silicon atoms at the surface layer have to be reorganized. It is obvious that the main shift is a horizontal displacement of the adatom. By doing this the Si_1–Si_2 bond overlap population will be reduced substantially. This is not a problem, since this bond is weak. The computed displacements of the Si atoms are listed in Table II.

Since the Si–O bonds are quite localized, it is safe to take Si–O distances and angles of oxygen from the structure of bulk SiO_2, with a mean value of 1.61 Å and 144° (Ref. 45) (Si–O–Si), respectively. In agreement with previous calculations[17,20] we have chosen these values for most cases. For the inserted oxygen it turned out that better results were obtained using an Si–O–Si angle of 140°, in agreement with Ciraci, Ellialtioglu, and Erkoc.[20]

TABLE II. Displacements of the Si atoms (in Å) for the case of an oxygen inserted in the Si_1–Si_3 backbond.

	Si1	Si3	Si4	Si5
x	+0.38	−0.11	−0.04	−0.04
y	···	···	+0.06	−0.06
z	+0.05	−0.22	−0.1	−0.1

A crucial point is the O–O distance. NEXAFS studies showed[46] that the O–O distance should either be 1.28 or 1.39 Å, depending on the way the experimental results are analyzed. Höfer *et al.* favor the shorter value because of expectations based on an O–O stretching frequency of 1230 cm^{-1}. According to Vaska,[47] one can assign reasonable values for O–O distances if one knows the charge on the coordinated molecule and vice versa. Based on this, the charge on the O_2 fragment we obtain from our calculations for most of the models (−1.2 to −1.6) is in better agreement with the longer distance of 1.39 Å. Also, Goddard, Redondo, and McGill have found an optimized distance of 1.37 Å for the *paul* configuration.

In Fig. 4 O_2 contributions to the DOS are shown for four O–O distances, for the *paul* configuration. Other configurations, such as *para*, *grif*, and *trival*, show very similar behavior.

To choose the right O–O distance, we can look at the splitting of the two O($2p$) levels depending on the distance. Since we know from UPS spectra that this splitting should be substantially bigger than 2 eV (otherwise one would see an additional peak), the shorter distance (1.28 Å) seems a more reasonable choice.

In the absence of a reliable geometry optimization, we have done all calculations with both distances (1.28 and 1.39 Å). If we do not explicitly mention the distance, we

mean the values depicted in Fig. 3, which, for most cases, is the shorter distance of 1.28 Å. Since most peroxo complexes have quite long O–O distances (mean value: 1.46 Å), we have chosen 1.39 Å for the *grif* configuration. In case of the *bridge* configuration, we had to lengthen the O–O bond to 1.5 Å and the Si–O bond to 1.78 Å. It is worth mentioning that such unusually long Si–O distances (bulk SiO_2 has Si–O distances of typically 1.61 Å) do occur in some Si–O complexes, which have distances between 1.65 and 1.79 Å.[45]

In case of *paul* and *para* the outer oxygen is above the hollow position. We discuss the (very small) threefold barrier due to rotation of the outer oxygen in a subsequent publication.[48]

In the different models for the precursor state, molecular O_2, stretched to a varying degree, is involved. It is thus appropriate to review the well-known orbitals of O_2, shown in structure 3 below (adapted from Ref. 49).

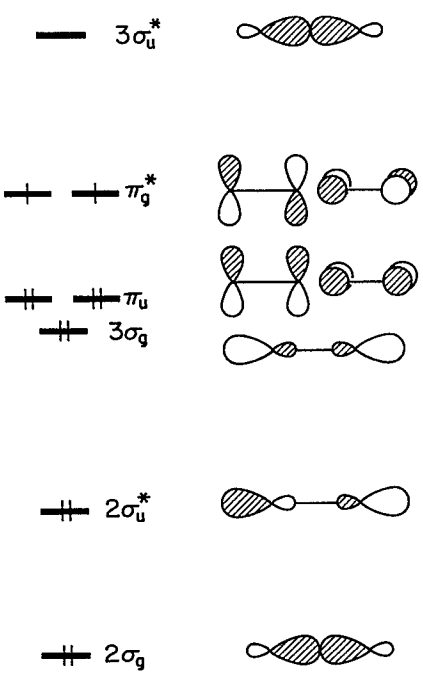

3

The ground state of O_2 is $^3\Sigma_g^-$, two electrons in the O–O antibonding π_g^* orbital. Superoxide, O_2^-, has a longer bond, corresponding to further filling of π_g^*, and peroxide, O_2^{2-}, has the π_g^* completely filled. Complexes of O_2 populate π_g^* to a varying extent[47,50] and are likely to span the range of distances between molecular O_2 (1.21 Å) and peroxide (typically 1.46 Å). In our coordinate system (see structure 1), the O (p_z)–O (p_z) interaction always belongs to the π set. But because the O_2 orientation varies, p_x and p_y have both σ and π character, or conversely one component of O_2 π may be made up of a mixture of p_x and p_y.

THE MOLECULAR PRECURSORS

Since temperature and coverage can change the kinetic channels for the O_2 molecules incident on the Si(111) surface,[15] different Si–O configurations should be expected depending on the experimental conditions. We concentrate on low O_2 exposures (e.g., 0.2 L O_2). There are two different temperature regimes: (a) room temperature, at which STM data were obtained (stage 1), and (b) low temperature (95 to 150 K), at which UPS, XPS, NEXAFS, etc. measurements were made. We try to separate these two regimes. We will see later that the main difference between the low- and the high-temperature configurations is due to a higher percentage of dissociated oxygen species formed at high temperatures.

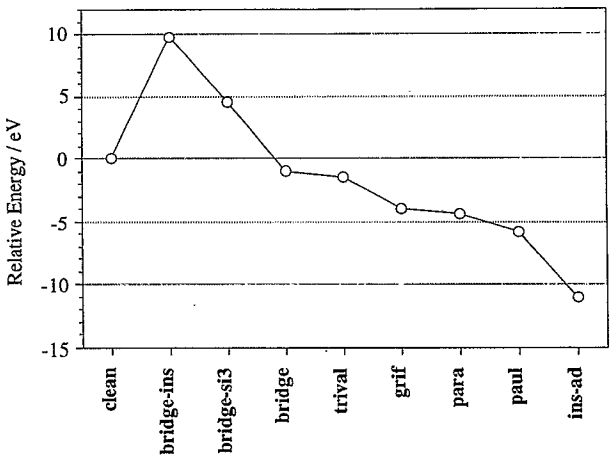

FIG. 5. Relative total energies of all molecular precursors mentioned and for the configurations *clean* and *ins-ad* (see Fig. 3). Since *bridge-ins* involves *three* oxygen atoms, this total energy is corrected by the energy the system gains by inserting one oxygen atom into the Si–Si backbond.

Before we summarize the findings for the two temperature regimes separately we discuss (I) total energies, (II) oxygen DOS in comparison with UPS spectra, (III) DOS close to Fermi energy in comparison with STM results, (IV) charges, (V) COOP for all molecular precursors.

(I) Figure 5 shows the relative total energies of all molecular precursors mentioned in the preceding section. For comparison, we have also shown the total energy for the clean surface plus an oxygen molecule (labeled *clean* in Fig. 3) and for the configuration *ins-ad* (stable and dominant Si–O configuration in the dissociated stage[51]).

This figure is consistent with the observation that most of the molecular precursors are metastable. The comparison to *clean* allows us to get an idea of the binding energy. For *grif*, *para*, and *paul*, the binding energy is substantial (~5 eV/unit cell). For a Si_3 cluster Goddard, Redondo, and McGill[17] calculated a binding energy of 2.2–2.5 eV for *paul* (1.37 Å). This indicates that an oxygen molecule, once it has hit the Si surface and found one of these positions, will stick there and await further dissociation. Figure 5 suggests that more than one molecular precursor may be involved in the oxidation process. Only two bridge configurations are significantly less stable, which can be explained easily in terms of unfavorable interactions (see discussion below).

The *ins-ad* atomic oxygen configuration is by more than 5 eV/unit cell preferred over all molecular precursors. This shows again the great thermodynamical tendency for

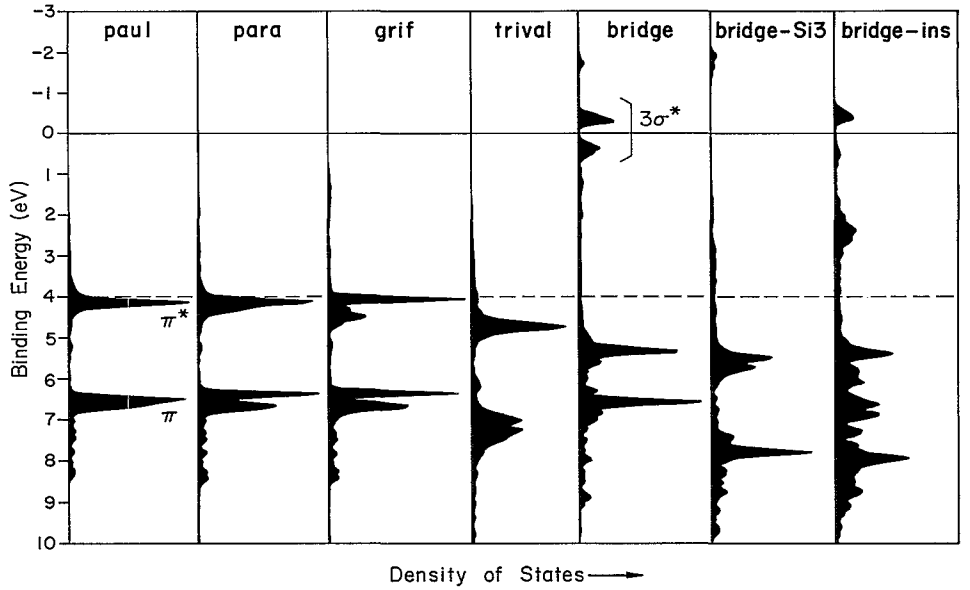

FIG. 6. Oxygen DOS for the precursors. The nature of some localized peaks is also indicated. All geometrical data can be obtained from Fig. 3. For *grif*, the O–O distance is also 1.28 Å.

the oxygen molecule to dissociate on the surface. The relatively long lifetime (10 min at room temperature) is due to kinetic barriers for the dissociation of the spectroscopically detectable precursors.

(II) Figure 6 shows DOS plots of the oxygen involved in these precursors, in order of descending total energy. Most of the DOS is very localized (this was pointed out already by Goddard, Redondo, and McGill).[17] One can clearly identify the original levels of the O_2 molecule (compare to structure 3). The indicated nature of the states reflects the *main* contributions to each peak. The π^* levels are not totally occupied. This can be deduced also from the charge of the O_2 fragment, which is not -2 but -1.2 to -1.6. The experiments indicate that the main spectroscopically detectable precursor has a DOS peak at 4 eV. This is demonstrated by comparing UPS spectra at 100 K (peak at 4 eV) and after annealing at room temperature (much smaller peak at 4 eV or no peak at all, as in Fig. 11).

We suggest that the second oxygen peak which results from the splitting of the O_Π levels be associated with the "7 eV peaks" which are already identified as belonging to the stable state that follows the dissociation of the precursor. Thus, by coincidence, the 7 eV peaks belong to both the precursor and the stable state. This is consistent with the fact that the intensity of the 7 eV peaks is never smaller than the 4 eV peak [see, e.g., the curve 0.1 L in Fig. 11(b)]. Others have interpreted this fact as indicating the inability—even at very low temperatures—to detect only the precursor without the stable state being mixed in to the extent of at least 50%. XPS data have been interpreted making the same assumption (see the Appendix for details).

Other calculations have also assigned the 4 eV peak to molecular oxygen species on the surface (π_g^*) and they agreed that these states are very localized and have a character similar to that of free O_2. For the other states, Chen, Batra, and Brundle[18] computed both the π_u and the $3\sigma_g$ levels to be at 10 eV instead of 7 eV. This would imply a stronger peak at 10 eV (π_u plus $3\sigma_g$) than at 4 eV (π_g). Such a strong 10 eV peak does not appear in the experimental UPS spectra (e.g., Ref. 15 or Fig. 11). Goddard, Redondo, and McGill[17] found the π_u peak at 7 eV and the $3\sigma_g$ peak at about 10 eV.

As can be seen from Fig. 6, *paul*, *para*, and *grif* have states at $\sim$4 and $\sim$7 eV below the Fermi level and thus fit best the UPS spectra. The *bridge* configuration shows too small a splitting of the oxygen levels, due to the long O–O distance of $\sim$1.5 Å. As discussed in the preceding section, this small splitting is not in agreement with the UPS spectra.

(III) The comparison of oxygen DOS with UPS spectra provides information about the nature of the Si–O structures formed at low temperature. In order to compare with room temperature STM results (stage 1) one must consider all possible DOS close to the Fermi energy.

(a) Some oxygen DOS is shifted close to the Fermi energy for the *bridge* configuration, which would give bright sites in STM images.
(b) If one considers Si atoms, the orbitals that could give bright STM images are mainly the adatom and rest atom dangling bonds (namely the corresponding p_z orbitals).

In Fig. 7 the DOS close to the Fermi energy of (a) the p_z (Si_1) (adatom) and (b) the p_z (Si_9) orbitals (rest atom) are shown for the various oxidation models. As expected, all direct interactions with the dangling bonds (for *paul*, *para*, and *grif*) shift them to higher energy. In some cases these are shifted too far from E_F to be detectable by STM. Thus, these precursors can only appear as dark sites in

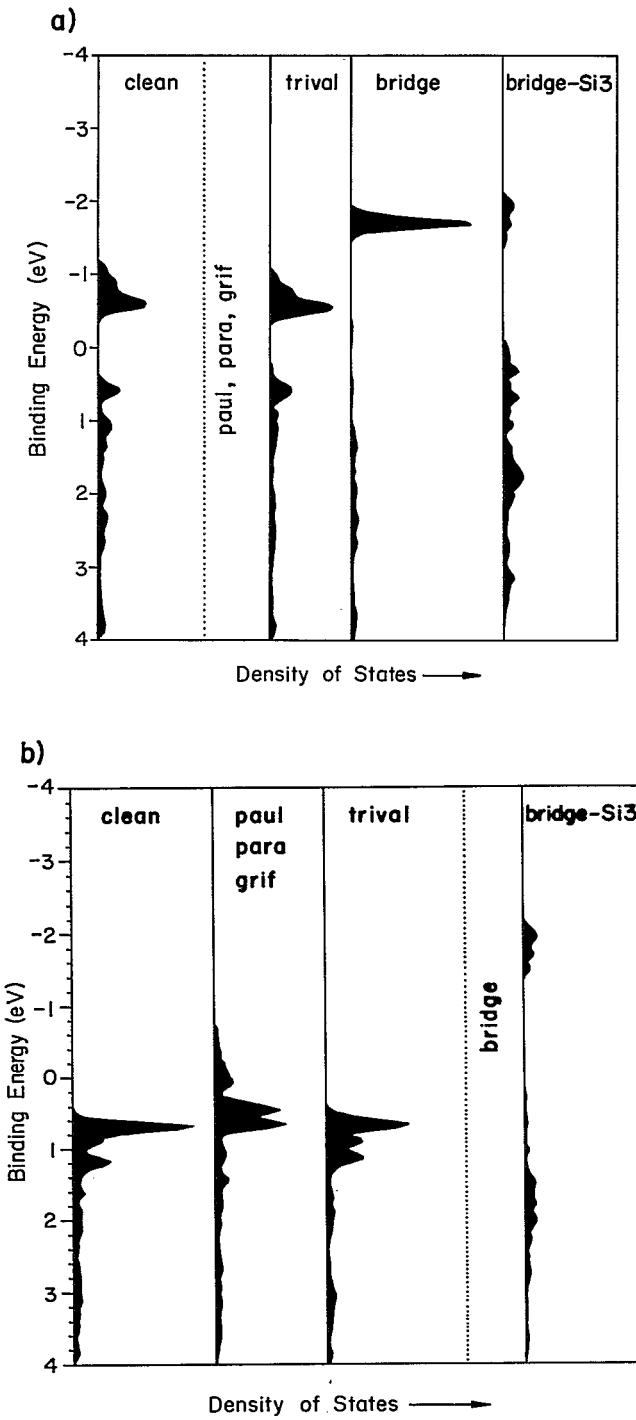

FIG. 7. DOS for the adatom p_z orbitals (a) and for the rest atom p_z orbital (b) for the configurations as indicated. All geometrical data can be obtained from Fig. 3. A dotted line indicates too small a DOS to be visable on this scale. In these cases the DOS is pushed up to higher energies due to O–Si_1 (p_z) interactions. The relative scale for the DOS is the same for all configurations.

STM. However, in the case of an indirect interaction (the oxygen *not* occupying an on top site; in *bridge* and *trival*) significant DOS remains near E_F, sufficient to lead to the appearance of bright sites in STM. STM indicates that early after small O_2 exposures (stage 1) about 50% of all reacted adatom sites appear bright.

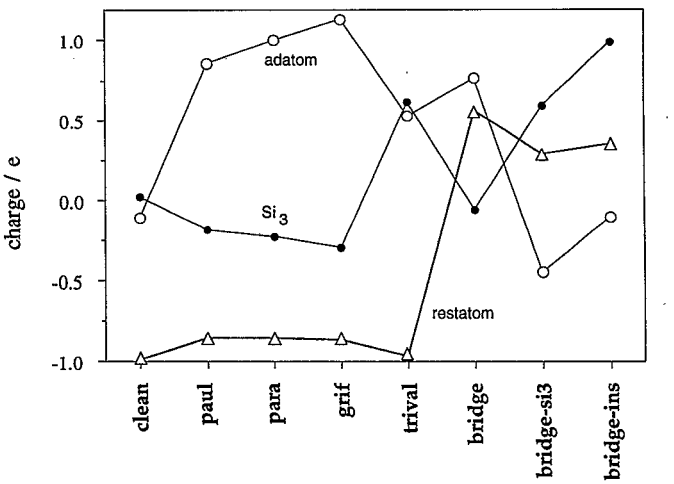

FIG. 8. Charges at different atoms for the configurations marked; open circle: adatom; solid circle: Si_3; triangle: rest atom.

(IV) Another measure of the energy shift of a state (e.g., a dangling bond) is the charge. If, as consequence of interaction, the DOS is pushed up in energy above the Fermi level, the corresponding occupation of that orbital is reduced and the charge on the atom becomes more positive (see also structure 4). In cases such as *paul*, *para*, and *grif* the occupied orbital which is pushed up in energy has mainly Si_1 p_z character (see structure 4, right picture).

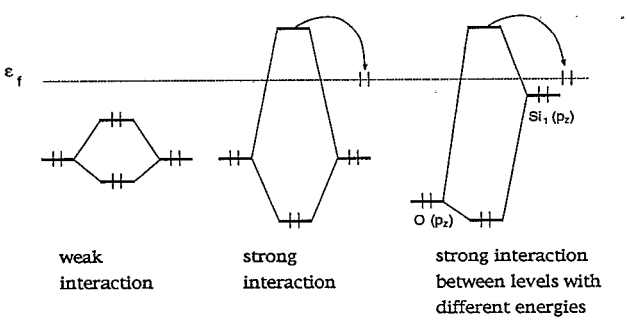

4

Figure 8 shows the charges at the adatom (Si_1), the Si_3 atom, and the rest atom (Si_9), for the precursors and for *clean* as a comparison. In general, these curves reflect the fact that the more charge is transferred, the stronger the silicon–oxygen interaction. In the cases of *paul*, *para*, and *grif*, basically all of the charge is transferred from Si_1 to the O_2, the very negative rest atom remains remarkably unaffected. For *trival* (for geometry see Fig. 3) the oxygen interaction with Si_1 and Si_3 is very similar. They give up an equal amount of charge density to the inserted oxygen. The rest atom dangling bond remains intact (see also Fig. 7). In *bridge* the rest atom gives much more charge to the oxygen than the adatom.

On the clean surface the rest atom is much more negative than the adatom. This is because the rest atom is unstrained; its dangling bond is near the top of the valence band, but not much destabilized. The adatom p_z orbital

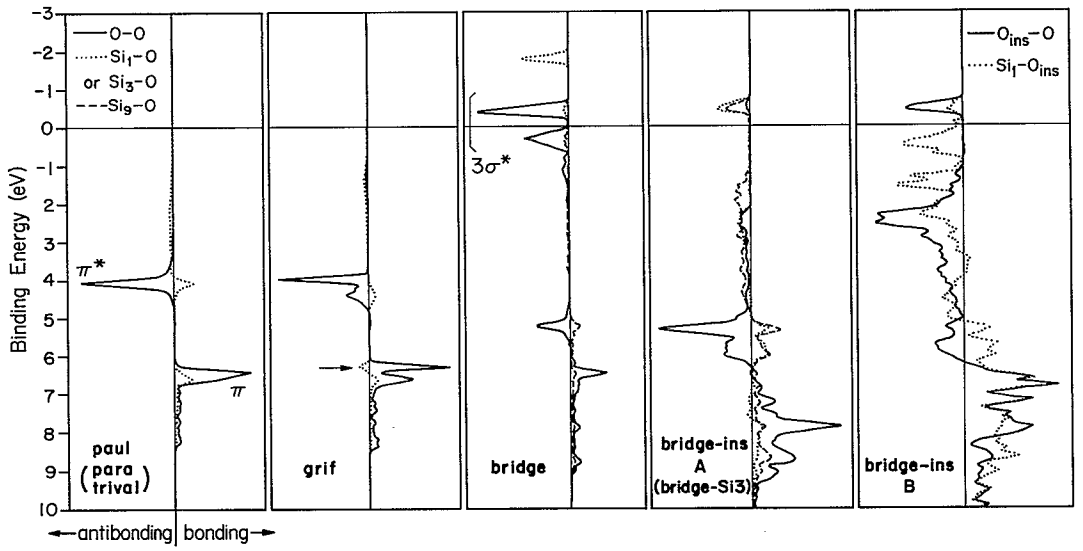

FIG. 9. COOP curves for the bonds between O–O (solid line); Si_1–O [Si_3–O for *bridge-si3* and *bridge-ins* (A)] (dotted line) and Si_9-O (dashed line). In *bridge-ins* (B) O_{ins}–O (solid line) and Si_1–O_{ins} (dotted line) is displayed.

interacts with the Si beneath so that the corresponding level is destabilized, and is pushed above the Fermi level.

(V) Figure 9 show the corresponding COOP curves for the O–O, Si_1–O, Si_3–O (*bridge-si3* and *bridge-ins*), Si_9–O and Si_1–O_{ins} bond. In the case of O_2 the states corresponding to the two O(2*p*) DOS peaks have quite different bonding characteristics. The lower one is bonding (labeled π) and the upper one is O–O antibonding (π^*). The molecular binding properties are maintained upon O_2 adsorption (see structure 3). This bonding–antibonding pattern is followed throughout all models. We have plotted the corresponding total overlap populations in Fig. 10(a).

For most configurations the π,π^* system of the oxygen molecule is retained despite the interaction with the surface (compare also to structure 3; note that the indicated levels in Figs. 6 and 9 reflect the main contributions for the peaks). The bond is, however, strongly weakened. The overlap population drops from 0.71 (O_2 in the gas phase with the *same* distance: 1.28 Å) to a bit below 0.5 [Fig. 10(a)]. As can be seen from Fig. 10(a) the overlap population for the bridge configuration drops sharply. This happens because the $3\sigma^*$ state is lowered in energy and part of its DOS is now below E_F (Figs. 6 and 9). To demonstrate the range of total overlap population for the O–O bond in *bridge* we have marked two data points in Fig. 10, one for the geometry shown in Fig. 3 and a second one for longer distances (Si–O: 1.8 Å, O–O: 1.53 Å). The fact that the overlap population is close to zero or even negative is an important result, since it shows that if bridge is formed as an intermediate on the Si(111) surface, it should immediately dissociate. Thus, bridge is an unlikely candidate for the main precursor, which is stable for ten minutes at room temperature.

Most of the Si–O overlap populations [Fig. 10(b)] are close to the "normal" value in SiO_2. One exception is *grif*. The reduced overlap population must be due to the geometry of the three-membered ring, which gives rise to stronger antibonding interactions. Indeed, one bonding peak becomes antibonding while going from *paul*, *para* to *grif*. This peak is indicated by an arrow in Fig. 9.

On the basis of the above results we can examine which of the molecular oxygen adsorption configurations are the most promising candidates for the precursor state.

(1) *Bridge-ins:* The reason why we consider this structure is that Höfer *et al.*[15] suggested that *bridge* will quickly dissociate leading to an inserted oxygen. They suggested that the O_2 could bond to Si_3 and Si_9 as in *bridge-ins*, to give a almost symmetrical structure with the O_2 axis parallel to the surface. This configuration appears to be ruled out by our calculations. Due to the unfavored O_{ins}–O interaction (Figs. 9 and 10) and to the presence of the hypervalent Si_3 atom, the system is unstable; its total energy is calculated to be almost 10 eV more positive than for the unreacted surface (Fig. 5). Moreover, the oxygen DOS (Fig. 6) does not match the peaks found experimentally.

(2) *Bridge-si3:* One of the destabilizing features of *bridge-ins* is the O_{ins}–O interaction. This interaction is not present in *bridge-si3*. From a geometrical point of view the O–O bridge fits well in between Si_3 and Si_9 (Fig. 3). But this configuration also can be ruled out: The total energy is 5 eV too high (probably due to the hypervalent Si_3).

(3) *Bridge:* This configuration can be ruled out, too: Figures 9 and 10 show that the long O–O bond (1.5 Å) in *bridge* is very weak and would dissociate instantly. Thus, *bridge* is an unlikely candidate for the main precursor, which is stable for 10 min at room temperature. Only at very low temperature could the *bridge* configuration be reasonably stable. However, even at low temperature *bridge* is unlikely to be present because the long O–O distance leads to a splitting of the oxygen DOS of only 1.2 eV—too small compared to the observed splitting of 3 eV (100 K UPS).

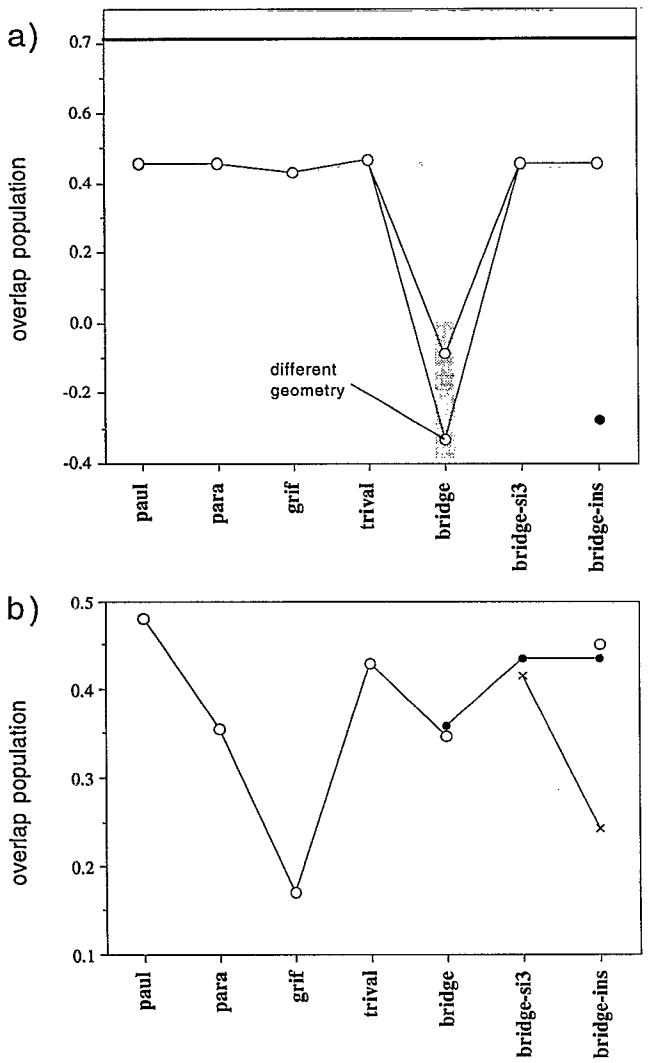

FIG. 10. Overlap populations for the precursors. (a) O–O: open circles; O_{ins}–O: solid circles; (b) Si_1–O: open circles; Si_9–O: solid circles; Si_3–O: crosses. The reference dark line in (a) indicates the overlap population for an oxygen molecule (1.28 Å) in the gas phase. The two data points for *bridge* reflect the influence of geometrical changes (see text).

We would like to mention at this point that the theoretical calculations of Kunjunny and Ferry,[52] which Höfer *et al.*[15] relied on and which show oxygen DOS in good agreement with the experimental results, were performed for an *unreconstructed* Si(100) surface which allows a symmetric peroxo bridge with a distance of only 1.28 Å. We do not believe that these DOS are of a bridge-type configuration that can be formed on the reconstructed Si(111) surface.

(4) *Trival:* This precursor configuration can probably be ruled out, too, at least in the case of low-temperature experiments. Experiments at 100 to 120 K have shown that the O–O axis has much more parallel than perpendicular character.[46] So, the *trival* structure with an angle of 60° to the surface (Fig. 3) cannot contribute significantly to the population of the spectroscopically detectable precursors at low temperature.

(5) *Grif:* So far, this structure cannot be ruled out. One possible objection is that a distance of 1.28 Å is a bit too short for this three-membered ring structure. A distance of 1.39 Å would lead to a splitting of the oxygen DOS too small to the one observed in UPS.

(6) *Paul:* The only argument for this structure not being the main precursor at 100 K is that the O–O axis makes an angle with the surface of 36° (Fig. 3) while NEXAFS experiments (at 100 K) show that this axis should be essentially parallel to the surface. Since all other data fit very well with experiment, we do not exclude this structure. At higher temperatures *paul* appears to be a very good candidate for the precursor.

(7) *Para:* This configuration appears to be in best agreement with experimental results and should definitely be considered a good candidate for the main precursor.

To summarize, only *grif*, *paul*, and *para* remain likely candidates for the *major*, metastable precursor. This is in agreement with the conclusion of Goddard, Redondo, and McGill[17] (they favored *paul*, 1.37 Å) and of Chen, Batra, and Brundle[18] (they favored *para*, 1.2 Å). The *paul* and *para* structures are similar. The former fits the experimental finding that the O–O axis is parallel to the surface, the latter has a lower total energy by 1.5 eV. We are driven to combine these structures, to form a *paul-para* hybrid. By mixing this two configurations we take into account some dynamics of the oxygen molecule chemisorbed on the Si(111) surface. This is illustrated in structure 5. Perhaps *grif* could be included, too.[53]

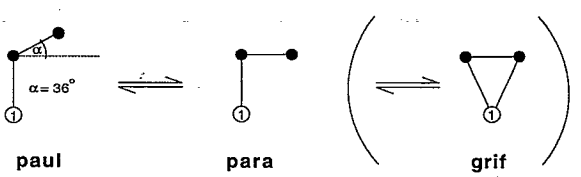

5

But not all experimental observations can be explained by choosing these molecular precursors. STM pictures at stage 1 (room temperature) indicate that ~50% of the reacted adatom sites appear as stable bright sites in STM topographs of unoccupied states. Such products cannot be obtained from *paul-para* or *grif* precursors. Moreover, UPS spectra indicate that the rest atom dangling bonds are, at least partly, eliminated by the interaction with oxygen. For these reasons, we might expect that other unstable precursors, which dissociate too fast to be detected with UPS, might be important in the oxidation process.

Candidates for these unstable and minor precursors are *trival* and *bridge*. Mainly due to the antibonding O–O bond in *bridge* (Figs. 9 and 10), this structure cannot be stable at room temperature. But it could be the unstable candidate, since *bridge* will dissociate to *ins-rest*, which gives rise to bright sites *and* eliminates the rest atom dangling bond.

So, we will add to the *major* precursors *grif* and *paul-para* the *minor* precursor *trival* (due to NEXAFS measurements[46] only the room temperature case) and the main product *ins-rest* produced by the *unstable* precursor *bridge* [see also structure 6 and paper II (Ref. 54)]. By including

structures like *ins-rest* we get a mixture of precursor and stable states, which is in agreement with experimental findings.

At this point we would like to discuss the room-temperature case first and the low-temperature case in a following part of this section. The results for both temperatures are similar. The main difference is that the ratio of precursor to dissociated state is a bit larger at 100 K.

Room-temperature conditions

The picture which fits best the product distribution formed in stage 1 (e.g., 0.2 L O_2, room temperature), is a mixture of roughly 50% (*ins*, *ins-rest*, *trival*) and 50% (*paul-para*, *grif*, *ins-ad*). The channels leading to this distribution are illustrated in structure 6. Bold names or arrows indicate favored configurations or pathways. See also paper II.

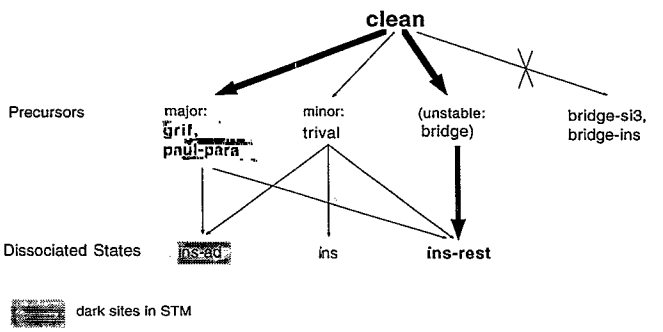

6

In order to give a strong UPS signal at 4 eV, *paul-para* and *grif* must be present in substantial amounts. In order to have approximately 50% *stable bright* sites in STM and to involve the rest atom (UPS finding), *ins-rest* should be the second dominant configuration.

To summarize, our calculations suggest that at low coverages at room temperature, initially a mixture of very roughly 40% *ins-rest*, 10% *trival*, 45% *paul-para* and *grif* and 5% *ins-ad* is formed (these percentages refer to the reacted sites. 90% of all sites will still be unreacted, i.e., *clean*). Please note that these percentages are merely intended to help us to visualize the processes occurring in stage 1. They are not to be taken as quantitative results. Taking this mixture of configurations, the ratio between bright sites and dark sites is 1:1, the ratio between adatom and rest atoms involved is 2.5:1, the mixture between precursors and stable states is 1.2:1. The resulting DOS's fit quite well the UPS spectra. All these facts are in good agreement with the UPS and STM experimental results. The dissociated configurations following these precursors also match the experimental results (see paper II).

Low-temperature regime

Figure 11 shows UPS ($h\nu$=40.8 eV) spectra[27] obtained by exposing the surface at 95 K to the indicated O_2 exposures, followed by brief annealing to the indicated

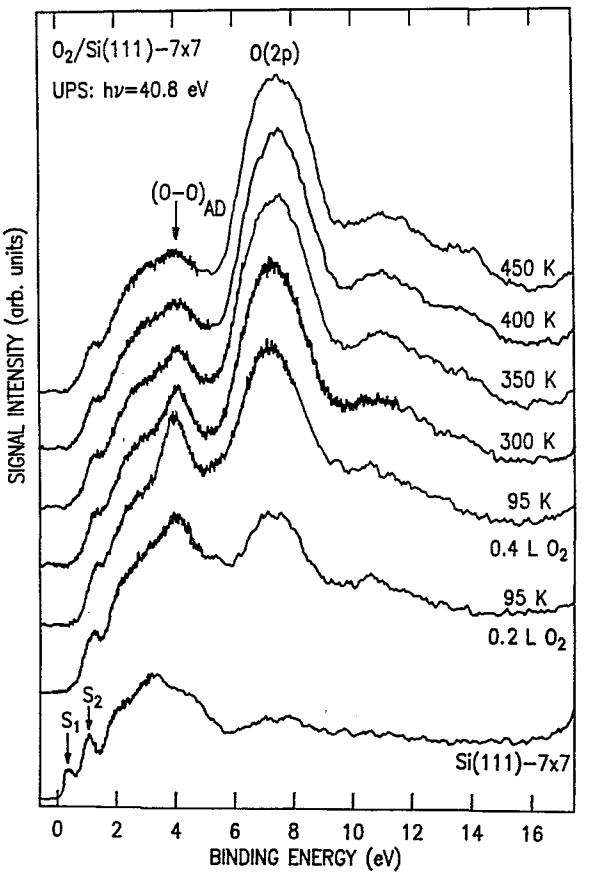

FIG. 11. UPS spectra of (a) the clean Si(111)–7×7 surface, indicating the adatom (S_1) and the rest atom dangling bond (S_2), (b) two different oxygen exposures to this surface at 95 K, (c) five different temperatures at 0.4 L O_2 to show the annealing process.

temperatures.[55] The spectra presented show best the preferential quenching of the adatom dangling bond at low oxygen exposure.

Let us consider two examples from the low- and high-temperature regimes: (a) 0.4 L, 95 K (precursor plus dissociated states), (b) 0.4 L, 300 K (only dissociated states).

Before we attempt to simulate the low-temperature regime, one should recall the results of the preceding sections. At low coverages (0.2 L O_2), stage 1, *room temperature*, we suggested as likely 45% (*grif* and *paul-para*), 10% *trival*, 40% *ins-rest*, and 5% *ins-ad*. Mixing these configurations in proportion to their weight, we would *not* get a good representation of stage 1 (precursor state), since STM pictures show that only about 10% of all adatom sites have reacted. In order to simulate this coverage we have to mix in 90% of the structure *clean*. The thus obtained DOS, however, does not compare well with the low-temperature UPS spectra, because the oxygen peaks are not strong enough, due to the presence of 90% of *clean*.

Since we get too much of *clean* surface character mixed in, it is reasonable to conclude that the coverage of oxygen containing sites at 95 K must be substantially higher at the same exposure. This is also indicated by, for example, the work of Ibach, Bruchmann, and Wagner[6] and

Nijishima *et al.*[16] They show that the sticking coefficient at 100 K is close to 1, approximately 10 times higher than at room temperature. The coverage, or more precisely, the fractional oxygen coverage, is defined as the ratio of the number of oxygen adatoms to the number of Si atoms in the first layer of the bulklike Si(111) surface.[16] The unreconstructed surface has 49 dangling bonds (7×7). However, the reconstructed surface has only 19 dangling bonds (12 at the adatoms, 6 at the rest atoms, and one at the corner hole). In other words, a coverage of about 0.4 is sufficient to quench all rest atom and adatom dangling bonds and a coverage of 0.25 to quench all adatom dangling bonds if the oxygen attacks the adatoms first (Fig. 11 and other results indicate that the adatom dangling bonds are initially preferentially quenched).

Let us now consider the reactions at rest atom sites. Most UPS spectra indicate that the rest atom peak at 1 eV does not change very much upon small oxygen exposures. But this does *not* imply necessarily that the rest atoms remain unreacted, because the adatom dangling bond of bright sites (inserted oxygen in the backbond) also has a DOS peak at about 1 eV.[51] So, upon rest atom reaction, bright sites may be created at the same time so that the 1 eV peak does not change too much. This situation may arise through the dissociation of the *bridge* precursor to give an *ins-rest* structure. The *ins-rest* configuration eliminates one rest atom dangling bond and creates a bright site at the same time.

To summarize, at 0.4 L (95 K), most of the adatom sites have reacted, most the rest atom dangling bonds are still intact, and the coverage is about 0.4. The reacted rest atoms most likely are the result of the formation of the *ins-rest* configuration.

Now, if we look at the configurations for stage 1 (STM), *room temperature* [90% *clean*, 4.5% (*grif* and *paul-para*), 1% *trival*, 4% *ins-rest*, and 0.5% *ins-ad*] it is obvious that the picture will be quite different at low temperature. First, we will *not* mix in *clean*, since a coverage of 0.4 corresponds to almost two oxygen atoms per 2×2 unit cell. Second, the presence of the *trival* structure in any significant amount is unlikely, since the O–O axis is found to be parallel to the surface at 95 K.

The configurations *grif*, *paul*, and *para* have very similar DOS, if one uses the 1.28 Å O–O distance for *grif*. Since the smaller distance is energetically not favorable for *grif*, we will concentrate on *paul-para*. Further, we get best agreement with the experimental results if we take a precursor:dissociated state ratio of 2:1. This reflects that at low temperature the dissociation probability is lower than at 300 K (this ratio was 1.2:1 at room temperature). Moreover, after reinterpreting the data of Höfer *et al.*[15] (see the Appendix) the same ratio of 2:1 results from the analysis of their XPS and UPS data.

This leaves us with 2/3 *paul-para* and 1/3 (*ins-rest* and *ins-ad*). The best fit with the UPS spectra is obtained for 2/3 *paul-para* and 1/3 *ins-rest*. The corresponding calculated DOS is shown in Fig. 12 (solid curve). Note that by doing this no adatom dangling bond states (at 0.5 eV) remain unchanged: They are either eliminated by interacting with an oxygen atom coming in on top (*paul-para*) or the dangling bond electrons are transferred to bright site dangling bonds (*ins-rest*), located at 1 eV. The combined rest atom plus bright sites peak is clearly seen, although shifted a bit to higher energies (compare to Fig. 11). The Si bands rise sharply up to 2 eV. This rise creates a shoulder at about 2 eV. In a polarized UPS study, Höfer *et al.*[15] observed such a peak at 2 eV. The peak at 4 eV is clearly attributed to the precursor and the peaks at ~7 eV are representative of a mixture of stable configurations and precursors.

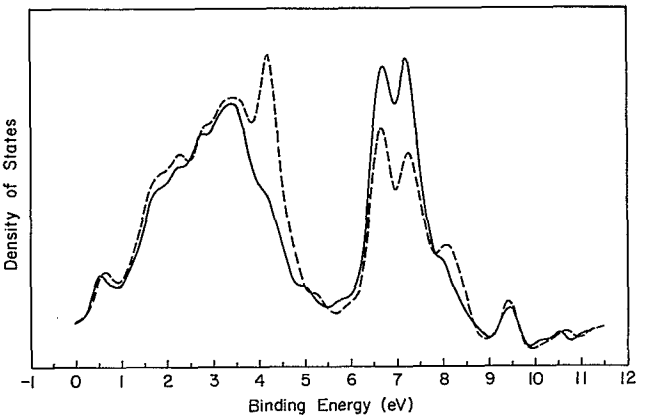

FIG. 12. Projected (and smoothed) DOS of the the adsorbate oxygen layer and the first two silicon double layers for (a) 67% *paul-para* and 33% *ins-rest* (solid line) and (b) 67% *ins-ad* and 33% *ins-rest* (dashed line).

After annealing to higher temperatures (no additional oxygen exposure) the precursor dissociates (see Fig. 11). At 95 K we have found the best fit for 2/3 *paul-para* and 1/3 *ins-rest*. This will give us 2/3 *ins-ad* (the main dissociation pathway for *paul-para*)[48] and 1/3 *ins-rest* at higher temperatures. The dashed line in Fig. 12 shows the corresponding calculated DOS. Note that the coverage is much higher than that in stage 2 (STM, room temperature). The reason is that we have exposed the surface to oxygen at 95 K and *then* we have annealed the surface. This leaves us with about 10 times higher surface coverage.

It is obvious from the experiments and calculations that the main change resulting from the dissociation of the precursor is a shift of DOS intensity from the 4 eV area to the 7 eV area. In both precursor and stable products the 7 eV band consists of mainly two peaks. In the Appendix we discuss some further details of the interpretation of the precursor states.

It needs to be mentioned that our approximate method of calculation neglects the image shifts of the negative ion states of O_2. This shift may be significant, and as a reviewer notes may increase charge transfer and the binding energies.

SUMMARY

As major stable precursors we have identified the *paul-para* and *grif* structures. A possible minor precursor is *trival* (only at room temperature). In addition, we have

considered the *bridge* configuration as an unstable precursor which dissociates immediately to give mainly the *ins-rest* structure. The remaining precursors give dark sites in STM pictures, and UPS signals at 4 and 7 eV, whereas the dissociated state *ins-rest* leads to bright sites and UPS signals at 7 eV. The ratio of precursor states:dissociated states is about 1:1 at room temperature and 2:1 at 100 K.

ACKNOWLEDGMENTS

We thank the Deutscher Akademischer Austauschdienst for the award of a NATO postdoctoral fellowship for B.S., and the Office of Naval Research for its support of the work at Cornell.

APPENDIX: FURTHER COMMENTS ON PRECURSOR STATES

In the studies by Höfer *et al.*[15] a single O (1*s*) XPS peak was obtained for the precursor state, whereas a peroxy radical should show a double peak.[56] It was suggested that this narrow O (1*s*) peak indicates that both oxygens are identical. It was mentioned that "the only alternative explanation would be that the second O (1*s*) peak accidentally coincides with the main O (1*s*) peak from the stable dissociated state," but this possibility was excluded by noting that a precursor to stable state ratio of 2:1 would be in disagreement with UPS results: Peaks 7 and 8 [7 eV peaks] only show a 50%, and not a 150%, increase after annealing of the mixed layer. However, as can be seen from Figs. 4 and 6, the precursor shows about the same DOS at 6 to 7 eV as at 4 eV. In other words, these peaks at 6.5 and 7.5 eV contain contributions from the DOS's of both the precursor and the stable state. A ratio of 2:1 (precursor:stable state) is in very good agreement with the UPS spectra: A 2:1 ratio means that the combined DOS for the peaks at 4 and 7 eV is distributed as follows (without 3σ contribution): 33% at 4 eV (precursor), 33% at 7 eV (precursor), and 33% at 7 eV (stable state). Taken together, 66% at 7 eV. By annealing, all precursor states change to stable states and we have now 100% at 7 eV. 100% as compared to 66% is a 50% increase, as it should be according to the UPS data. Another indication that this scheme may be correct is that the O (1*s*) peak from the stable state in the XPS spectra shifts a bit towards higher energy during annealing. Höfer *et al.*[15] found the splitting of this O (1*s*) peak to be 1.1 eV. This is close to the calculated splitting for a peroxy-radical [1.3 eV (Ref. 57)], which is a good argument in favor of our *paul-para* precursor structure.

The net effect of reinterpreting these experimental data is that (a) we do not need to accept any more that the two oxygens of the precursor are identical, (b) the 7 eV peaks result come from both, precursor states *and* stable states, and (c) it *is* possible to have almost exclusively precursor states at very low temperatures.

[1] J. T. Law, J. Phys. Chem. Solids **4**, 91 (1958).
[2] M. Green and K. H. Maxwell, J. Phys. Chem. Solids **13** 145 (1960).
[3] M. Green and A. Liebermann, J. Phys. Chem. Solids **23**, 1407 (1962).
[4] F. M. Meyer and J. J. Vrakking, Surf. Sci. **38**, 275 (1973).
[5] H. Ibach and J. E. Rowe, Phys. Rev. B **10**, 710 (1974).
[6] H. Ibach, H. D. Bruchmann, and H. Wagner, Appl. Phys. A **29**, 113 (1982).
[7] R. Ludeke and A. Koma, Phys. Rev. Lett. **34**, 1170 (1975).
[8] C. M. Garner, I. Lindau, C. Y. Su, P. Pianetta, and W. E. Spicer, Phys. Rev. B **19**, 3944 (1979).
[9] G. Hollinger and F. Himpsel, Phys. Rev B **28**, 3651 (1983); J. Vac. Sci. Technol. A **1**, 640 (1983).
[10] A. J. Schell-Sorokin and J. E. Demuth, Surf. Sci. **157**, 273 (1985).
[11] U. Höfer, P. Morgan, W. Wurth, and E. Umbach, Phys. Rev. Lett. **55**, 2979 (1985).
[12] G. Hollinger, J. F. Morar, F. J. Himpsel, G. Hughes, and J. L. Jordan, Surf. Sci. **168**, 616 (1986).
[13] M. Leibsle, A. Samsavar, and T.-C. Chiang, Phys. Rev. B **38**, 5780 (1988).
[14] P. Morgan, V. Höfer, W. Wurth, and E. Umbach, Phys. Rev. B **39**, 3720 (1989).
[15] V. Höfer, P. Morgan, W. Wurth, and E. Umbach, Phys. Rev. B **40**, 1130 (1989).
[16] K. Edamoto, Y. Kubota, H. Kobayashi, M. Onchi, and M. Nishijima, J. Chem. Phys. **83**, 428 (1985).
[17] W. A. Goddard III, A. Redondo, and T. C. McGill, Solid State Commun. **18**, 981 (1976).
[18] M. Chen, I. P. Batra, and C. R. Brundle, J. Vac. Sci. Technol. **16**, 1216 (1979).
[19] A. S. Bhandia and J. A. Schwarz, Surf. Sci. **108**, 587 (1981).
[20] S. Ciraci, S. Ellialtioglu, and S. Erkoc, Phys. Rev. B **26**, 5716 (1982).
[21] G. Binnig, H. Rohrer, Ch. Gerber, and E. Weibel, Phys. Rev. Lett. **49**, 57 (1982).
[22] R. Hamers, Annu. Rev. Phys. Chem. **40**, 531 (1989).
[23] G. Binnig, H. Rohrer, Ch. Gerber, and E. Weibel, Phys. Rev. Lett. **50**, 120 (1983).
[24] R. J. Hamers, R. M. Tromp, and J. E. Demuth, Phys. Rev. Lett. **56**, 1972 (1986).
[25] Ph. Avouris and R. Wolkow, Phys. Rev. B **39**, 5091 (1989).
[26] K. Takayanagi, Y. Tanishiro, M. Takahashi, and S. Takahashi, J. Vac. Sci. Technol. A **3**, 1502 (1985).
[27] Ph. Avouris, I.-W. Lyo, and F. Bozso, J. Vac. Sci. Technol. B **9**, 424 (1991).
[28] R. Hoffmann, *Solids and Surfaces: A Chemist's View of Bonding in Extended Structures* (VCH, New York, 1988).
[29] T. Hughbanks and R. Hoffmann, J. Am. Chem. Soc. **105**, 1150 (1983).
[30] R. Hoffmann, J. Chem. Phys. **39**, 1397 (1963).
[31] M.-H. Whangbo and R. Hoffmann, J. Am. Chem. Soc. **100**, 6093 (1978); R. Hoffmann, Rev. Mod. Phys. **60**, 601 (1988).
[32] J. H. Ammeter, H.-B. Bürgi, J. C. Thibeault, and R. Hoffmann, J. Am. Chem. Soc. **100**, 3686 (1978).
[33] J. E. Northrup, Phys. Rev. Lett. **57**, 154 (1986).
[34] H. Tokumoto, K. Miki, H. Murakami, H. Bando, M. Ono, and K. Kajimura, J. Vac. Sci. Technol. A **8**, 255 (1990).
[35] J. P. Pelz and R. H. Koch, Phys. Rev. B **42**, 3761 (1990).
[36] R. D. Meade and D. Vanderbilt, Phys. Rev. B **40**, 3905 (1989).
[37] I. K. Robinson, W. K. Waskiewicz, P. H. Fuiss, and L. J. Norton, Phys. Rev. B **37**, 4325 (1988).
[38] G.-X. Qian and D. J. Chadi, Phys. Rev. B **35**, 1288 (1987).
[39] J. E. Northrup, Phys. Rev. Lett. **57**, 154 (1986).
[40] As a test of the validity of our approach we have compared our predictions on the relative stability of the adsorption configurations of boron on Si(111) with the results of first principles calculations. It was shown (see Ref. 41) that boron first occupies the T-4 position [preferred over the H-3 (hollow) position], but the thermodynamically stable configuration consists of a B substitutional atom directly below a Si adatom at a T-4 site. This site is called S-5. Our calculations show the same order of total energy: S-5 < T-4 < H-3. The energy differences are of the order of 1–2 eV unit cell.
[41] P. Bedrossian, R. D. Meade, K. Mortensen, D. M. Chen, J. A. Golovchenko, and D. Vanderbilt, Phys. Rev. Lett **63**, 1257 (1989); I.-W. Lyo, E. Kaxiras, and Ph. Avouris, *ibid.* **63**, 1261 (1989); R. L. Headrick, I. K. Robinson, E. Vlieg, and L. C. Feldman, *ibid.* **63**, 1253 (1989).
[42] From R. Ramírez and M. C. Böhm, Int. Quantum Chem. **30**, 391 (1986).
[43] From J. S. Griffith, Proc. R. Soc. London, Ser. A **235**, 73 (1956).
[44] End-on model from L. Pauling, Nature (London) **203**, 182 (1964).

[45] A. F. Wells, *Structural Inorganic Chemistry*, 4th ed. (Clarendon, Oxford, 1975).
[46] U. Höfer, A. Puschmann, D. Coulman, and E. Umbach, Surf. Sci. **211/212**, 948 (1989).
[47] L. Vaska, Acc. Chem Res. **9**, 175 (1976).
[48] B. Schubert, D. Proserpio, and R. Hoffmann (unpublished).
[49] T. A. Albright, J. K. Burdett, and M.-H. Whangbo, *Orbital Interactions in Chemistry* (Wiley, New York, 1985).
[50] A. B. P. Lever and H. Gray, Acc. Chem. Res. **11**, 348 (1978).
[51] I.-W. Lyo, Ph. Avouris, B. Schubert, and R. Hoffmann, J. Phys. Chem. **94**, 4400 (1990).
[52] T. Kunjunny and D. K. Ferry, Phys. Rev. B **24**, 4593 (1981).
[53] *Paul-para* should not be viewed as a time average of *paul* and *para*—but as a dynamic intermediate with less defined bond angle and bond length (see also Ref. 48).
[54] B. Schubert, P. Avouris, and R. Hoffmann, following paper, J. Chem. Phys. **98**, 7606 (1993).
[55] Taking advantage of polarization differences, some workers have been able to resolve two peaks at 6.5 and 7.5 eV [see, e.g., Höfer *et al.* (Ref. 15)], whereas others have found one peak at 7 eV.
[56] A. Redondo, W. A. Goddard III, C. A. Swarts, and T. C. McGill, J. Vac. Sci. Technol. **19**, 498 (1981).
[57] M. Fujita, H. Nagayoshi, and A. Yoshimori, Surf. Sci. **242**, 229 (1991).